Adsorption and Desorption of an O_2 Molecule on Carbon Nanotubes

Xiao Yan Zhu,[1] Seung Mi Lee,[1] Young Hee Lee,[1,2,*] and Thomas Frauenheim[3]

[1]*Department of Semiconductor Science and Technology, Jeonbuk National University, Jeonju 561-756, Korea*
[2]*Department of Physics and Semiconductor Physics Research Center, Jeonbuk National University, Jeonju 561-756, Korea*
[3]*Universität-GH Paderborn, Fachbereich Physik, Theoretische Physik, 33095 Paderborn, Germany*

(Received 22 February 2000)

Adsorption and desorption of an oxygen molecule on carbon nanotubes are investigated using density functional calculations. Several precursor states exist at the edge of armchair nanotubes, whereas an exothermic adsorption takes place at the edge of zigzag nanotubes. We also estimate desorption barriers of a CO molecule from nanotubes as well as fullerenes and amorphous phases. Our calculations suggest that carbon nanotubes can survive selectively during the oxidative etching process with a precise control of annealing temperature, in good agreement with experimental results of purification process of carbon nanotubes.

PACS numbers: 61.48.+c, 68.45.Da, 81.65.Mq, 82.30.−b

Since the discovery of carbon nanotubes (CNTs) from arc discharge in 1991 [1], great efforts have been done for the synthesis of CNTs in massive quantity and their purification processes. Electric arc discharge of graphite rods has been considered to be an appropriate method for the synthesis of CNTs in large quantity [2,3]. However, with these approaches a large quantity of unnecessary carbonaceous particles such as fullerenes, nanoparticles, and amorphous (a-) phases are always contained in the soot in addition to the CNTs [4,5]. Highly purified CNTs are in general required for further sophisticated measurements and practical applications.

Purification involves in general the separation and the elimination processes of some carbonaceous particles from CNTs. Various standard techniques such as filtration, chromatography, and centrifugation, have been tried for the purification [6]. The key step for the purification process is an oxidative etching in gas-phase reaction or liquid-phase reaction in an acidic solution [6]. All these processes presume the fact that the oxidative etching takes place selectively between CNTs and other carbonaceous particles; i.e., the oxidative etching rate of the carbonaceous particles is faster than that of CNTs. Although the CNTs are separated from those particles to some extent, some particles still remain in the purified samples and, moreover, the purification yield is poor in most cases [6]. Understanding the adsorption and desorption of an O_2 molecule for CNTs and the carbonaceous particles is prerequisite in order to improve the yield during the purification process. The main difficulty of understanding such processes arises from the lack of a theoretical model in an atomic scale.

In this work, we have carried out a systematic study for adsorption and desorption of an O_2 molecule on CNTs using the density functional (DF) calculations. Some key intermediates are identified in the adsorption process. An O_2 molecule adsorbs on the nanotube wall and diffuses into the edge. We will show that several precursor states exist on the armchair edge, which may delay the onset of O_2 molecular adsorption, whereas an O_2 molecule dissociatively chemisorbs without an activation barrier on the zigzag edge. We also evaluate the desorption barriers of a CO molecule from the CNT edges in a concerted desorption pathway. We will prove that fullerenes and a-carbon can be oxidatively etched away more easily than CNTs due to lower desorption barriers, and therefore CNTs can survive selectively during the oxidative etching process.

For our calculations we use a self-consistent charge density-functional-based tight-binding (SCC-DFTB) method [7] and local atomic orbital (LCAO)-basis DF calculations [8] within local-density approximation (LDA) and generalized-gradient approximation (GGA).

We choose supercells of $(5, 5)$ armchair and $(9, 0)$ zigzag nanotubes in our calculations, with respective diameters of 6.8 and 7.0 Å and average bond lengths of 1.42 Å. Ten and eight layers along the tube axis (z axis) are chosen for armchair and zigzag nanotubes, respectively. We first calculate an O_2 adsorption on the CNT wall. The adsorption energy can be defined, $E_{\text{ad}} = E_{\text{tot}}(\text{O}_2 + \text{CNT}) - E_{\text{tot}}(\text{O}_2) - E_{\text{tot}}(\text{CNT})$, where E_{tot} is the total energy of a given system. We tried various adsorption sites for an O_2 molecule on both tubes [9]. The adsorption energies are ranged within $-0.5 - -0.6$ eV for all cases [10,11]. The O_2 molecular bond is not broken apart, with the bond lengths varying from 1.48 Å to 1.53 Å. Thus, the O_2 molecule adsorbs on the tube wall with a relatively small adsorption energy and migrates easily to the CNT edge.

We now calculate an O_2 adsorption at the CNT edges. We tried various adsorption positions with different orientations of an O_2 molecule. Several metastable (stable) states are found at the armchair edge, as shown in Figs. 1(a)–1(d). The O_2 molecule first adsorbs at the top site on the triply bonded C_2 dimer (bond length: 1.25 Å) [12], as shown in Fig. 1(a). The bond length of O_2 molecule is simply expanded from 1.10 to 1.57 Å, due to the Coulomb repulsion between two oxygen atoms, where the Mulliken excess charges ($-0.10e$) are accumulated. The C_2 dimer becomes double-bonded with a bond

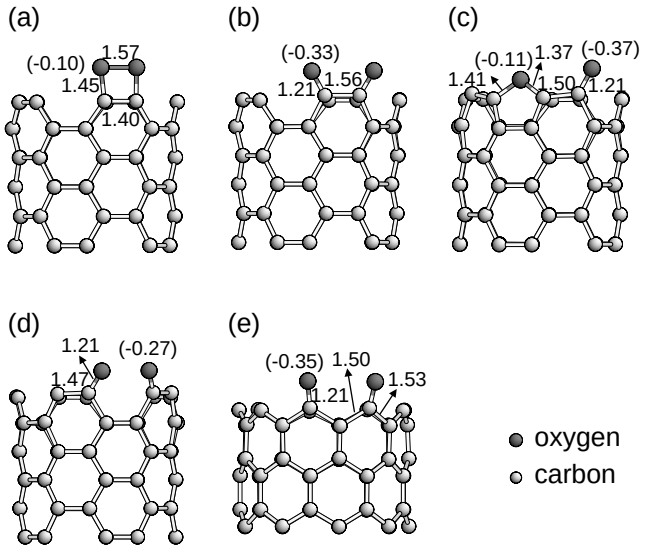

FIG. 1. Adsorption of an O_2 molecule on CNT edges: (a),(b) the intermediate states on the top site of the armchair edge, (c) the final state with oxygen atoms located at pentagon and top sites of the armchair edge, (d) the seat site of the armchair edge, and (e) the top sites at the zigzag edge. The dark and grey balls indicate the oxygen and carbon atoms, respectively. All bond lengths are in units of Å. The Mulliken excess charges of the oxygen atoms are shown in parentheses in units of electron.

length of 1.40 Å, and the weak CO bonds are formed. The adsorption energy of this configuration is -4.04 (-4.61:-3.82) eV from SCC-DFTB (LDA:GGA) calculations. Another intermediate state is obtained by separating the O-O distance a little. After full relaxation, the O-O bond is now completely separated, as shown in Fig. 1(b). A more significant amount of charge transfer ($-0.33e$) is observed in this case. The C-O bond strengths become stronger with bond lengths of 1.21 Å, and the C_2 dimer is single-bonded now. This gives rise to the stronger adsorption energy of -7.41 (-7.81:-6.89) eV. The energy barrier between these two precursor states is only 0.11 eV. A more stable configuration is obtained by separating the O-O distance further, as shown in Fig. 1(c). One oxygen atom is located at the pentagon site with weak C-O bonds (bond lengths: 1.41 and 1.37 Å), and the other oxygen atom is at the top site with a strong C-O bond (bond length: 1.21 Å). The O-O distance is far apart by 2.81 Å. This configuration is the most stable one among others with an adsorption energy of -7.98 (-8.13:-7.04) eV. Note that the relative energy changes between intermediate states are similar, independent of the different calculational approaches. The energy barrier from Figs. 1(b) and 1(c) is 0.73 eV. We find another stable configuration, where the O_2 molecule adsorbs at the seat site, as shown in Fig. 1(d). A strong Coulomb repulsive force exists between two oxygen atoms, separating the O-O bond and resulting in the relatively low adsorption energy of -5.26 eV.

Unlike the armchair edge, where several intermediate states exist, the adsorption of an O_2 molecule at the zigzag edge shows only one available top site, independent of initial orientations and positions of an O_2 molecule, as shown in Fig. 1(e). The O_2 molecule simply dissociates first without any energy barrier and then chemisorbs on two adjacent top sites, forming strong C-O bonds with bond lengths of 1.21 Å. The energy gain is larger with an adsorption energy of -8.39 eV. This is expected, since the edge energy of a zigzag CNT is higher by 0.8 eV than that of armchair CNT [12,13].

We also calculate the adsorption of O_2 on the fullerene and *a*-carbon, which remain with CNTs in a large portion of the pristine soot. Figure 2(a) shows an intermediate state of O_2 adsorbed at the top site on a double bond (hexagon-hexagon:*h*-*h*) of C_{60}. The O-O distance is kept to 1.52 Å, with C-O bond lengths of 1.50 Å. The C-C bond becomes single-bonded, showing similar trends to previous reports [14,15]. The adsorption energy is -1.68 eV, relatively smaller than those of CNT edges. Breaking up the O-O bond length to 2.50 Å [Fig. 2(b)] requires a potential barrier of 1.57 eV. However, this enhances the adsorption energy to -3.25 eV. Note that this process already opens the cage structure, as shown in Fig. 2(b). With further oxidation, the cage is expected to be fragmented easily with even lower barrier height. We find another adsorption site at top site on a single bond (pentagon-hexagon:*p*-*h*), which gives smaller adsorption energy of -0.86 eV than that on the double bond. The transition from this precursor state to the final geometry [Fig. 2(d)] requires a smaller barrier height (0.71 eV) than that on the *h*-*h* bond. The

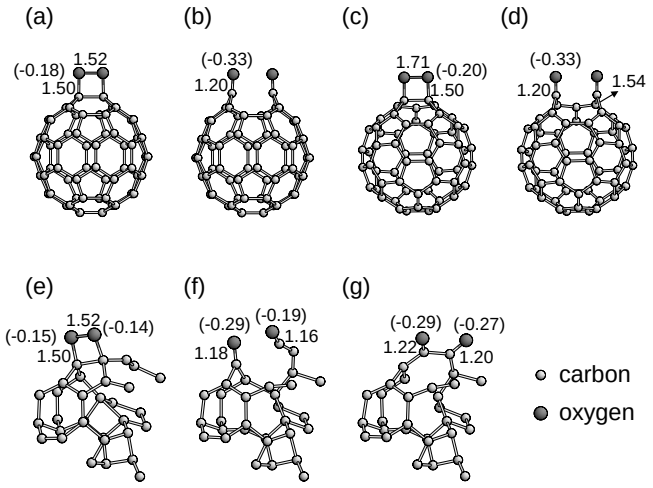

FIG. 2. Adsorption of an O_2 molecule on carbonaceous particles: (a) a precursor state on the *h*-*h* bond of C_{60}, (b) the final state on the *h*-*h* bond of C_{60}, (c) a precursor state on the *p*-*h* bond of C_{60}, (d) the final state on the *p*-*h* bond of C_{60}, (e) the initial O_2 adsorption on top of the C_3-C_3 bond of *a*-surface before relaxation, (f) the fully relaxed on-top configuration of the C_3-C_3 site, and (g) the fully relaxed geometry of the O_2 adsorption on top of the C_2-C_3 site. All other notations are the same as in Fig. 1.

local atomic geometries are similar to the adsorption on the h-h bond. The adsorption energies are determined by the available π electrons.

For an adsorption of O_2 on a-carbon surface, we first generated a-carbon network using melting-quenching molecular-dynamics simulation technique [10,16]. In the supercell 144 carbon atoms were used to generate a-carbon network with periodic boundary conditions. The periodic boundary condition along the z axis was then removed to open the a-carbon surface and annealed again at 1000 K, followed by the quenching process, until the forces on each atom were less than 0.01 a.u. Only one twofold coordinated atom was present on the surface and the rest of the atoms were threefold coordinated, i.e., mostly graphitized [10]. Various adsorption sites have been tested. Figure 2(e) shows the typical local intermediate geometry when an O_2 molecule adsorbs on top of the C_3-C_3 site, where C_n stands for an n-fold coordinated atom. In this case, the O-O bond is not broken, similar to the local structure of the precursor states in C_{60}. The adsorption energy is -2.36 eV, within the range of the energy gain by the adsorption on the single bond (-1.68 eV) and the double bond (-3.25 eV) in C_{60}. Separating the O-O bond leads to the final configuration, as shown in Fig. 2(f). This process requires a barrier height of 0.36 eV but the energy gain is high with strong C-O bonds and the strain release, resulting in the adsorption energy of -11.0 eV. Figure 2(g) shows the typical local geometry of an O_2 molecule adsorbed on top of the C_3-C_3 bond. In this case, the O_2 molecule dissociates first without an activation barrier and adsorbs on the surface with strong C-O bond with bond lengths of about 1.2 Å. This involves one C-C backbond breaking, but more strain energy is involved during the relaxation, resulting in a large adsorption energy of -11.7 eV. Thus, the adsorption of the O_2 molecule on the a-carbon surface is strongly site dependent with relatively large adsorption energy. We expect O_2 molecules more likely to be adsorbed on a-carbon than fullerenes and nanotube edges.

So far, we have carried out energetics of O_2 adsorption on various species. In order to describe the oxidative etching, we evaluate a desorption barrier of a CO molecule from the adsorbed phases, which governs the kinetics of the system. Although various geometries are energetically stable, we choose the one which is energetically most stable in a given phase. For armchair edge, we choose the configuration given in Fig. 1(c) as a starting configuration for desorption, as shown in Fig. 3(a). We first try to desorb the C-O pair from the pentagon site. The corresponding potential barriers for concerted pathways are shown in Fig. 4. We move up the carbon atom below the oxygen atom at the pentagon site by 0.2 Å along the z axis and then fix the z coordinate of the chosen carbon atom. The C-O bond becomes stronger as the carbon atom moves away from the edge. The barrier height of 2.48 eV is observed at the step (iii), where the C-O pair loses the bond

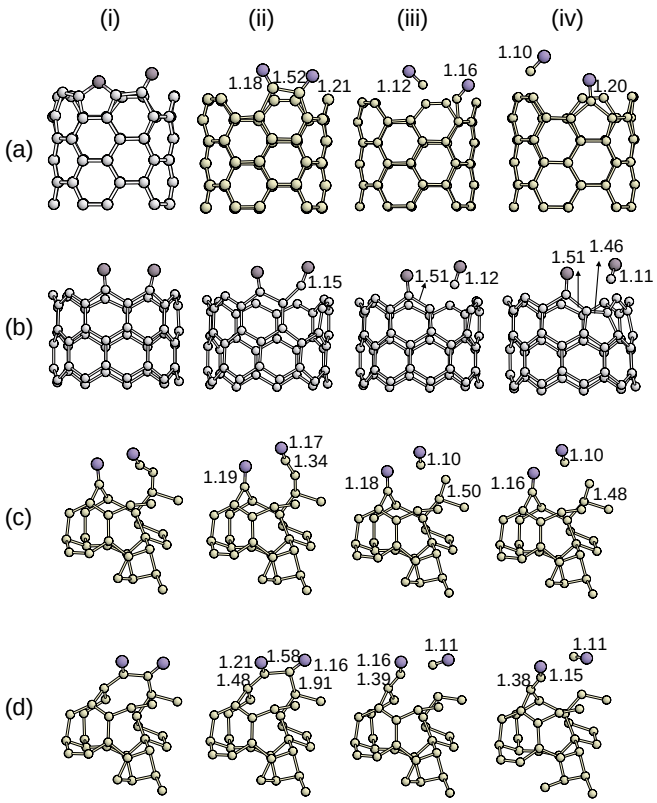

FIG. 3. Desorption pathways of the C-O pair from (a) the pentagon site at the armchair edge, (b) the top site at the zigzag edge, (c) the on-top of the C_3-C_3 bond on the a-surface, and (d) the on-top of the C_2-C_3 bond on the a-surface. All other notations are the same as in Fig. 1.

with the adjacent carbon atoms. The oxygen atom at the next top site rebonds to the carbon atoms at the pentagon site, gaining the energy by 2.0 eV. One may imagine the desorption of the C-O pair from the top site first. However, this requires relatively large barrier height of about 4.0 eV [10]. Desorption pathways from the zigzag edge are relatively simple, as shown in Fig. 3(b). We move up the carbon atom below the oxygen atom, similar to the previous calculations. Two C-C bonds are broken one by one,

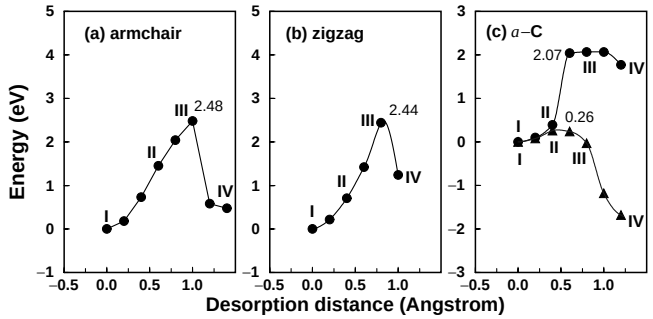

FIG. 4. The desorption energy barrier of CO from given pathways in Fig. 3; (a) the pentagon site at the armchair edge, (b) the top site at the zigzag edge, and (c) on-top of C_3-C_3 bond (filled circles) and on-top of C_2-C_3 site (filled squares) on amorphous surfaces. The corresponding pathways are indicated in Fig. 3.

showing the barrier at the step (iii) with the barrier height of 2.44 eV. The lone carbon bonds are again backbonded, forming a pentagon which has an energy of 1.2 eV. This barrier height is similar to that of the armchair edge.

For desorption barriers of the C-O pair from the a-carbon surface, various pathways can be chosen. Figures 3(c) and 3(d) show the pathways which give the minimum barriers, and the corresponding barriers are given in Fig. 4(c). The desorption barrier from the C_3-C_3 site [Fig. 3(c)] is 2.1 eV, as shown in the step (iii), where most energy cost results from the bondbreaking of strong C-C bond. In case of desorption from the C_2-C_3 site [Fig. 3(d)], the barrier height is 0.25 eV, relatively low due to two weak C-C bonds (1.58 and 1.91 Å). The desorption energy barrier was found to vary from 1 to about 2 eV, depending on the site. The desorption will take place from the site which requires the smaller activation barrier.

We now discuss the selective etching by O_2 oxidation, based on our calculations. Armchair CNTs have several precursor states with small activation barriers before reaching the final stable configuration, as shown in Figs. 1(a)–1(c). This may delay the onset of O_2 adsorption at the armchair edge. Adsorption on the zigzag edge is exothermic without any precursor state and gains larger energy than that on the armchair edge. A selective etching between armchair and zigzag tubes may be observed by controlling etching time. The desorption barrier of the C-O pair from the zigzag edge is about the same as that from the armchair edge. This suggests that it is difficult to observe a selective etching between these two CNT edges. In case of fullerenes, despite the smaller adsorption energies, the cage structures can easily be broken by continuous supplies of O_2 molecules, as discussed in Figs. 2(a)–2(d). The energy gain for O_2 adsorption on a-phase is very large, although the desorption barriers vary significantly from site to site. The etching will take place from the site which gives smaller activation barrier first. Therefore, the fullerenes and the a-phase can be easily etched away first by the selective etching. Controlling annealing temperature during thermal treatment is very crucial. One may estimate the annealing temperature from the Redhead's equation [17], $E_A/K_BT_d = \ln(\alpha T_d) - \ln(E_A/K_BT_d)$, where α is a constant and dependent on coverage, rate constant, and heating rate. Assuming the first order kinetics, one may obtain a reasonable desorption temperature (T_d) for a given activation barrier (E_A). The estimated desorption temperatures of the C-O pair from armchair edge, zigzag edge, C_{60}, and a-phase are 953, 937, 273, and 100 K, respectively, for the corresponding desorption barriers of 2.48, 2.44, 1.18, and 0.26 eV. Considering the fact that DF calculations usually underestimate the activation barriers, these values are reasonably good agreements with experimentally observed annealing temperatures of near 1050 K for CNTs [18,19]. Precise control of the annealing time is also necessary in order to get a high yield of CNTs.

In summary, we have investigated the reaction of an O_2 molecule with CNTs using DF calculations. The O_2 molecule arriving at the tube wall does not adsorb on the wall and instead glides into the edges. Several precursor states exist on an armchair edge, which may delay the onset of O_2 adsorption, whereas the O_2 molecule exothermally dissociates and chemisorbs at the zigzag edge. Desorption processes of the C-O pair are also investigated with concerted pathways in order to study the kinetics. Desorption barriers of the C-O pair from the fullerenes and the a-surface are significantly lower than those from the CNT edges. By comparing adsorption energies and desorption barriers of CNTs with those of fullerenes and a-carbon, we show that a selective etching can occur such that CNTs can survive during thermal treatment under an oxygen ambient.

We acknowledge the financial support by the MOST through NRL program, the KOSEF through the QSRC at Dongguk University, and in part by the BK21 program.

*Author to whom correspondence should be addressed. Email address: leeyh@sprc2.chonbuk.ac.kr

[1] S. Iijima, Nature (London) **354,** 56 (1991).
[2] S. Iijima and T. Ichihashi, Nature (London) **363**, 603 (1993).
[3] D. S. Bethune *et al.,* Nature (London) **363**, 605 (1993).
[4] D. T. Colbert *et al.,* Science **266**, 1218 (1994).
[5] Y. Ando and S. Iijima, Jpn. J. Appl. Phys. **32**, L107 (1993).
[6] T. W. Ebbesen, *Carbon Nanotubes: Preparation and Properties* (Chemical Rubber, Boca Raton, 1997).
[7] M. Elstner *et al.,* Phys. Rev. B **58**, 7260 (1998).
[8] DMol is a registered software product of Molecular Simulations Inc.
[9] The convergency criterion for structure optimization is that all forces acting on the atoms be $\leq$0.001 a.u. for all cases except for a-carbon, where the maximum forces are chosen to be 0.01 a.u.
[10] X. Y. Zhu and Y. H. Lee (unpublished).
[11] The adsorption on the defective tube wall is more stable than this. For instance, see M. S. C. Mazzoni *et al.,* Phys. Rev. B **60**, R2208 (1999).
[12] Y. H. Lee *et al.,* Phys. Rev. Lett. **78**, 2393 (1997).
[13] D.-H. Oh and Y. H. Lee, Phys. Rev. B **58**, 7407 (1998).
[14] I. G. Batirev *et al.,* Chem. Phys. Lett. **262**, 247 (1996).
[15] M. Menon and K. R. Subbaswamy, Chem. Phys. Lett. **201**, 321 (1993).
[16] E. Kim and Y. H. Lee, Phys. Rev. B **49**, 1743 (1994).
[17] R. I. Masel, *Principles of Adsorption and Reaction on Solid Surfaces* (John Wiley & Sons, Inc., New York, 1996), p. 513.
[18] Y. S. Park *et al.* (unpublished).
[19] T. W. Ebbessen and P. M. Ajayan, Nature (London) **358**, 220 (1992).